Proceedings of ASME Turbo Expo 2011
GT2011
June 6-10, 2011, Vancouver, British Columbia, Canada

GT2011-45173

DETAILED CHARACTERISATION OF A SWIRLED AIR/KEROSENE SPRAY IN REACTIVE AND NON-REACTIVE CONDITIONS DOWNSTREAM FROM AN ACTUAL TURBOJET INJECTION SYSTEM

Lecourt Renaud*
ONERA – The French Aerospace Lab
Mauzac, France

Linassier Guillaume
ONERA – The French Aerospace Lab
Toulouse, France

Lavergne Gérard
ONERA – The French Aerospace Lab
Toulouse, France

ABSTRACT

As part of the investigations of the ignition of jet-engines under altitude conditions, a detailed data base was built with the results of experiments on the two-phase flow produced by an actual swirl air/kerosene turbojet injection system. The injection system had a fairly simple geometry. It was used with liquid kerosene injected through a pressure-swirl fuel atomiser. In this case the measurements were carried out at atmospheric pressure in a windowed combustion chamber, with air at ambient temperature. The tested equivalence ratio was 0.95 which corresponds to an air mass flow rate of 0.035 kg/s. For this operating point, we obtained the velocity field of the gas phase under non-reactive conditions by LDA. The axial velocity component of the gas phase was also measured in the burning spray using an original method with a phase Doppler device. The data recorded with the PDA were also processed to obtain the kerosene droplet sizes and velocities under reactive conditions. The same phase Doppler device was used in non-reactive conditions to measure the size and velocity distributions of the kerosene droplets in a section close to the injection system exit in order to complete the data base with the boundary conditions for the liquid phase. In addition the flame was visualised qualitatively. The picture of the stabilized flame was processed with an Abel transform to compare the LDA/PDA measurements with the flame structure, obtained under the reactive conditions. Finally, unsteady pressure measurements were taken under non-reactive conditions and the LDA measurements processed, close to the injection system exit, to get the PVC (Precessing Vortex Core) frequency.

The data were analysed to determine the influence of the spray combustion on the two-phase flow. The geometry of the whole experimental setup and the data base are available to other researchers for testing and validating spray combustion models and unsteady two-phase flow numerical simulations.

INTRODUCTION

Because of forthcoming anti-pollution regulations and global warming, jet-engine manufacturers need to develop new designs for combustion chambers and injection systems. As the fuel is injected in liquid phase, engineers have to cope with many complex phenomena involved in spray combustion: atomisation, droplet interaction, vaporisation, mixing, combustion etc. which may be contradictory with the goals to be achieved, namely fuel efficiency, low pollution and thermal sustainability. Engineers are thus relying more and more on CFD flow simulations, for which the physical models first have to be validated. This validation requires comprehensive and well characterised and documented experiments. Such work has already been done for one-phase combustion at a laboratory scale, with the Sandia flames, [1, 2], and also with a more realistic setup such as the PRECCINSTA configuration, [3]. Reactive two-phase flows are more experimentally demanding and there are no comprehensive data bases with realistic configurations available for the moment. There are well documented experiments for which drop sizes, velocities and temperature, [4], even at elevated pressure, [5,6], were measured under reactive conditions. However the validation of spray combustion models requires quantitative measurements

* Corresponding Author; E-Mail: Renaud.Lecourt@onera.fr

such as of the gas-phase velocity or concentration field. In reference [5], the gas-phase velocity field was measured under isothermal conditions, without the presence of the spray and in reference [6], it was measured with the spray, under reactive conditions but without discrimination between the gas seeding particles and the fuel droplets. In reference [7], the authors produced a comprehensive data base for a reactive two-phase flow, but as the flow velocities were low, they could assume that there was no velocity slip between the gas and the small fuel droplets. Finally, Chrigui et al., [8], also tried to provide a comprehensive data base for a non-reactive evaporating spray. In addition to isothermal gas phase velocity measurements and drop size and velocity measurements, they used all of the information given by the Phase Doppler device to estimate the axial droplet mass flux. Although their results are in agreement with their CFD simulation of the two-phase flow, this is estimation and not a measurement. The present work describes a truly comprehensive data base on a burning spray. In addition to classical LDA/PDA measurements under isothermal and reactive conditions, to flame visualisation and unsteady measurements of pressure, the study included the velocity field (axial component) of the gas phase under reactive conditions, thus allowing the validation of spray combustion models.

EXPERIMENTAL SETUP

Test setup

The ignition tests were performed on the MERCATO (Moyen Expérimental de Recherche en Combustion Aérobie par Techniques Optiques[1]) test bench at ONERA Fauga-Mauzac.

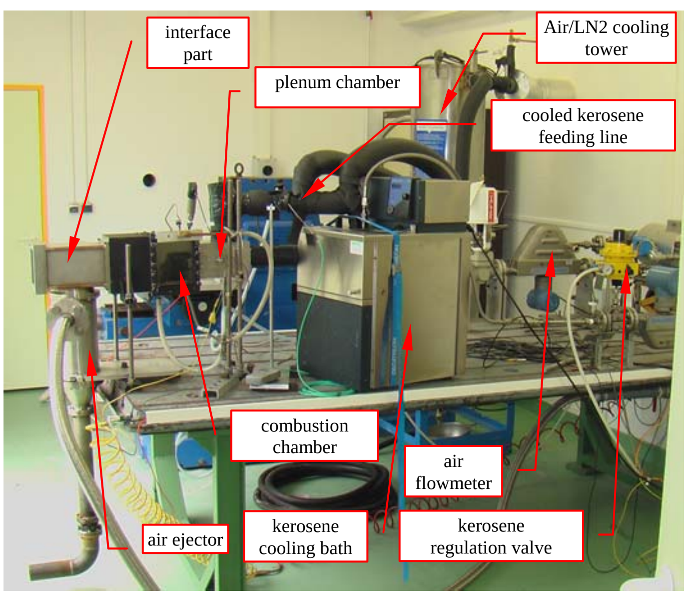

Fig. 1: MERCATO Test bench

[1] Experimental setup for investigation of air-breathing combustion using optical techniques

The bench was designed for two-phase flow analysis and operation of jet engine injection systems under conditions of actual low pressure and low air and kerosene temperatures. Fig. 1 shows a side view of the MERCATO test bench including labels for its major components. More details on the bench can be found in [9].

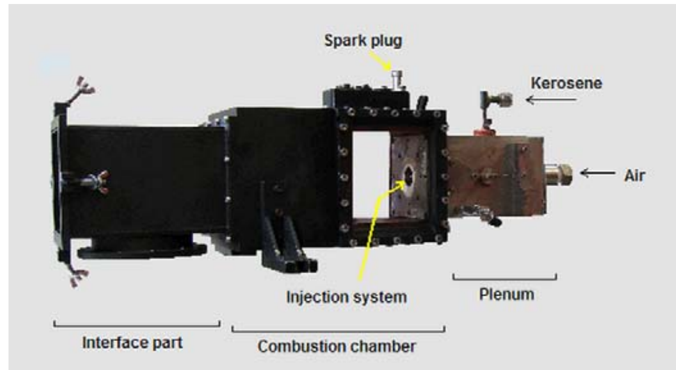

Fig. 2: Setup

The setup used for the experiments consists of a plenum chamber, containing the injection system, the combustion chamber itself and an interface assembly with an air ejector, Fig. 2. The test chamber's dimensions are 129mm x 129mm x 235mm. It can be fitted with lateral walls that can be replaced by windows to allow optical observation and measurements or by a carrier plate to mount a spark plug. The injection system (see Fig. 3) was provided by TURBOMECA. It is a radial swirler design with a pressure-swirl fuel injector.

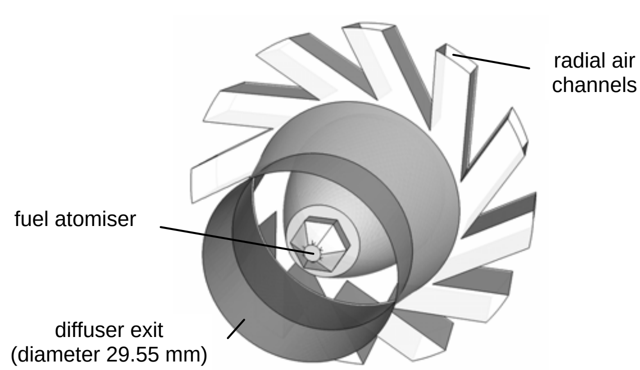

Fig. 3: TIMECOP Injector

Fig. 4 illustrates the reactive two-phase flow structure produced with such a setup. A laser sheet technique was used to visualise the liquid kerosene in the median longitudinal section of the chamber during a combustion test. The laser sheet was produced with a pulsed laser with pulse duration of a few tens of nanoseconds, which froze the flow movements. The picture was taken in the visible range, perpendicularly to the laser sheet, through a lateral window of the combustion chamber, Fig. 2. The injection system exit is on the left hand side of the picture and the air/kerosene mixture flows from left to right. The swirling two-phase flow produces a central recirculation zone and a corner/toroidal recirculation zone. The burning kerosene spray, illuminated in green by the laser sheet, expands between these two zones. Upstream, kerosene droplet and ligament groups are scattered by the turbulent eddies of the air flow. Downstream, the fuel is atomised in individual dispersed droplets (green spots). Finally, the kerosene is entirely evaporated before the end of the window at 130 mm from the injection system exit. Some liquid accumulated in the lower part of the combustion before ignition is also visible in this picture.

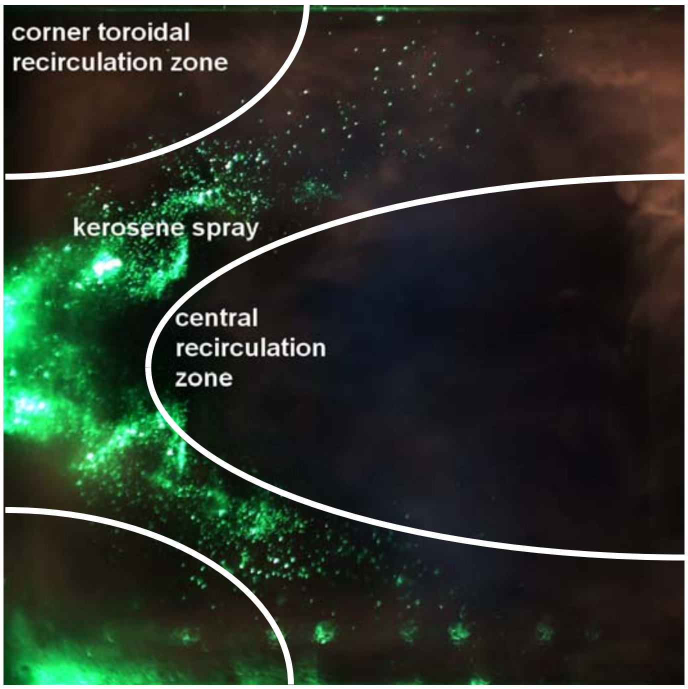

Fig. 4: Reactive two-phase flow structure

With the exception of the LDA measurements under non-reactive conditions, the two-phase flow was characterised at the reference operating point shown in table 1.

Operating point	reference	LDA
Pressure	1 atm.	1 atm.
Air flow rate	0.0350 kg/s	0.0199kg/s
Inlet Air temperature	293 K	463 K
Pressure drop	5.2 kPa	2.7 kPa
Swirl number	0.65	0.65
Kerosene flow rate	0.00225 k/s	
Equivalence ratio	0.95	

Table 1: Operating points

Measurements

We mainly performed LDA/PDA measurements, with a Phase Doppler Interferometer (PDI) from Artium. This device can measure two perpendicular velocity components. When the flow is axisymmetric, it is therefore possible to measure, Fig. 5, left hand side, the axial component (green arrows) and the tangential component (blue arrows) along a horizontal diameter of the flow (x axis), and the axial component (green arrows) and the radial component (blue arrows) along a vertical diameter of the flow (z axis). The LDA/PDA measurements were thus taken along perpendicular diameters in the square section of the combustion chamber. Thanks to the low value of the reception angle between the transmitter (TX) and the receiver (RX) for the LDA optical setup, these measurements were performed along almost the whole length of the diameters, Fig. 5, upper right hand side. On the other hand, the PDA optical setup requires a high reception angle, to collect the light scattered by the droplets in a dominant scattering mode (refraction or reflection) to enable correct signal processing. The measurements were therefore performed only along slightly more than a radius, Fig. 5, lower right hand side. The flow was characterised in this way in 5 sections of the combustion chamber, Fig. 6.

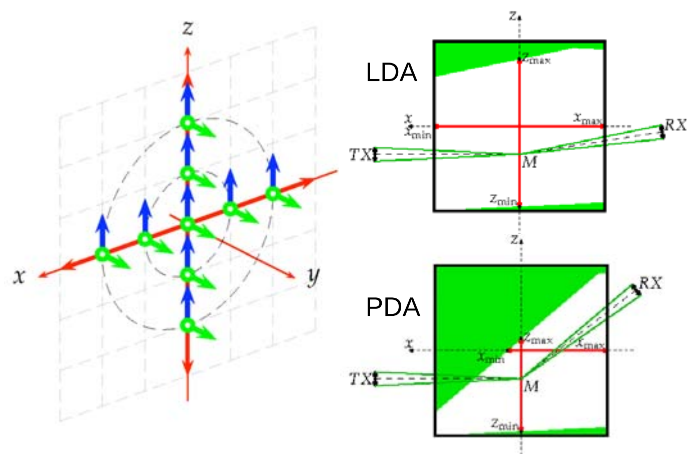

Fig. 5: LDA/PDA measurement configurations

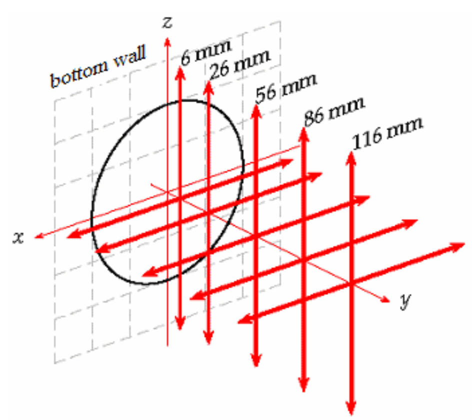

Fig. 6: LDA/PDA measurement sections

RESULTS

Non-reactive flow characterisation

A LDA characterisation of the gaseous flow was performed during investigation of the ignition phenomenon in aero-engines, [9]. The characterisation was carried out for specific operating points that had been defined for investigating ignition. It was therefore performed at atmospheric pressure and at an air temperature of 463 K, in order to reproduce the air density of altitude conditions (233 K, 0.5 atm.) and for 3 bulk velocities of the investigated domain. Olive oil droplets were used as seeding particles. The examples of results show clearly, Fig. 7 and Fig. 8, that the gaseous flow in the combustion chamber is exactly self-similar according to the bulk velocity. The similarity also exists for the RMS values of the velocity fluctuations. From these results, the velocity field, average and RMS of fluctuating values can validly be extrapolated for the reference operating point, the bulk velocity of which, 46.9 m/s, is only 12% higher than the highest bulk velocity, 41.85 m/s, of the LDA measurements.

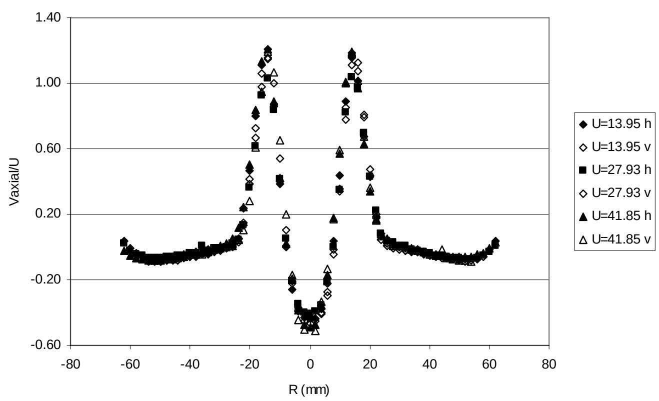

Fig. 7: LDA gas phase axial velocity, normalised by bulk velocity, in the 8 mm section

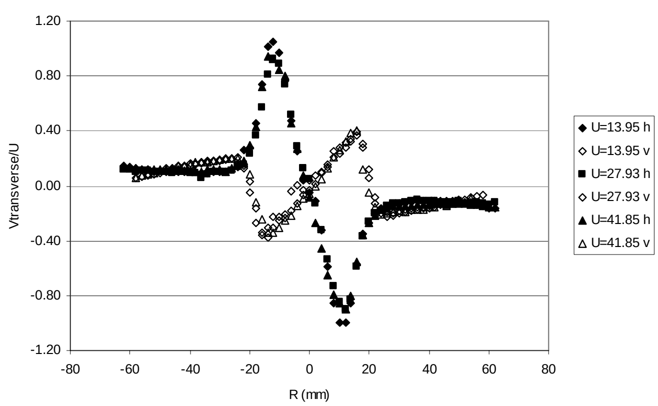

Fig. 8: LDA gas phase tangential and radial velocities, normalised by bulk velocity, in the 8 mm section

Then, to provide the liquid phase boundary conditions for the CFD specialists, we measured the drop sizes and velocities (3 components) as close as possible to the diffuser exit, i.e. in the 6 mm section. Fig. 9 shows the arithmetic mean diameter (D10) and the Sauter Mean Diameter (D32) profiles and Fig. 10, the mean value profiles of the 3 velocity components. The liquid volume flux and RMS velocity profiles are also available.

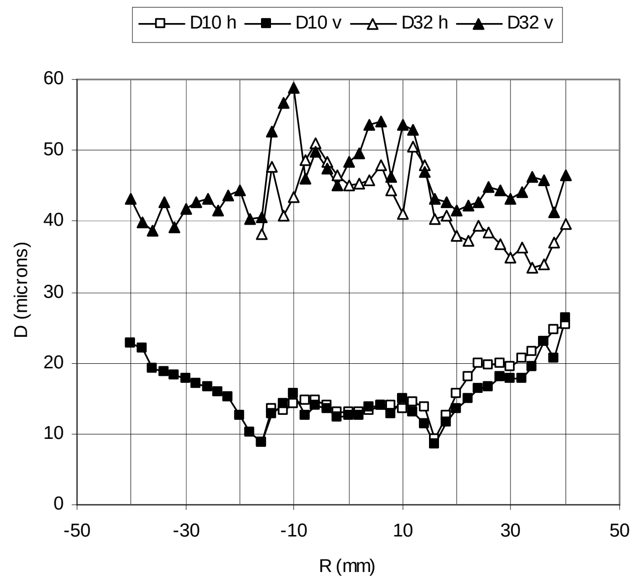

Fig. 9: Kerosene droplet sizes in the 6 mm section

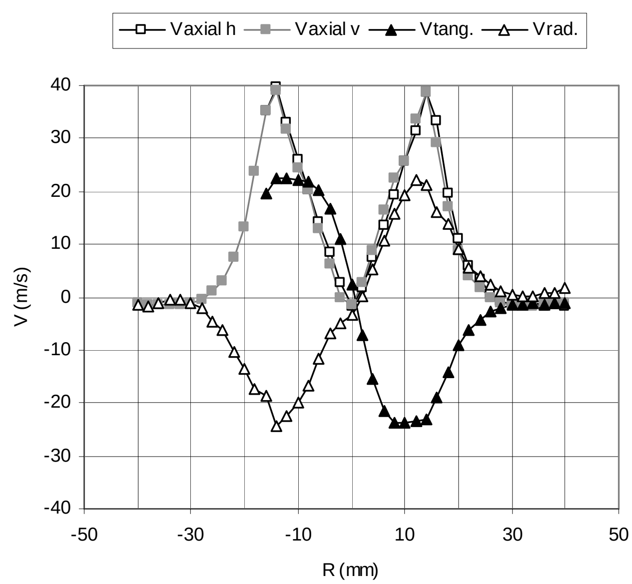

Fig. 10: PDA kerosene droplet velocity components in the 6 mm section

Finally, because CFD simulations of the cold gaseous flow, [10], had shown a strong PVC at the exit of the diffuser, always for the reference operating point, unsteady measurements of pressure were carried out with a microphone on the side wall of the combustion, 10 mm downstream from the injection face. The plot in Fig. 11 shows the power spectrum calculated from these unsteady measurements of pressure with a high peak at 1050 Hz. From the CFD computations, other spectra obtained for different bulk velocities and from the previous LDA measurements at the same operating point, [9], it is possible to state that it is the frequency of the PVC.

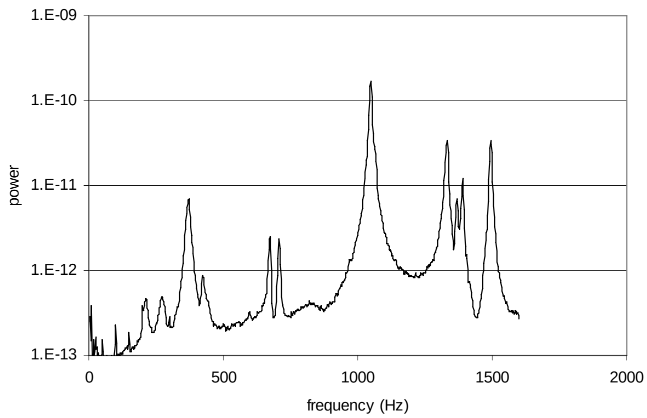

Fig. 11: Pressure power spectrum at combustion chamber lateral wall, in the 10 mm section

Reactive flow characterisation

Under reactive conditions, again for the reference operating point, an original method was developed to measure the axial velocity component of the gaseous phase, without assuming that there is no velocity slip between the small fuel droplets and the gas phase. Air was seeded with Zirconia particles, 80% of which were equal to or smaller than 3 micrometers in diameter. For such 1-3 micrometer particles, the Stokes number was estimated to be between 0.05 and 0.45. The particle and droplet velocities were measured with a Phase Doppler device, set to obtain the size information simultaneously. The results were then filtered according to size, to keep only the velocity measurements of particles and droplets smaller than 5 micrometers.

The method was checked for the cold flow case, especially to ascertain whether the Zirconia particles could be used to track the gas flow. The LDA measurement obtained with olive oil seeding was compared with Zirconia seeding, for the LDA configuration and the PDA configuration. We found a good agreement between the three measurements, except for the largest values, see Fig. 12, which proves that Zirconia particles track the gas phase velocity rather well. For the reactive case, if the Zirconia particles could be discriminated from kerosene droplets of the same size, we could then obtain the gas flow velocity in the burning spray.

Under reactive conditions, some of the reduced samples exhibited either quasi-monomodal or bimodal velocity distributions.

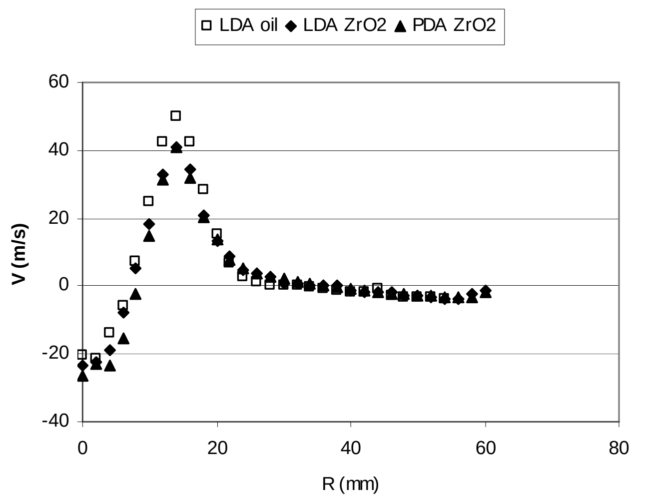

Fig. 12: Average velocity measurements under cold flow conditions at diffuser exit

In the example shown in Fig. 13, the velocity distribution reveals two peaks, at about 30 m/s and 70 m/s. For these kinds of samples, the velocity distributions were processed using the MIXMOD software [11], interfaced with Matlab©. This software offers different algorithms for processing density estimation, clustering or discriminant analysis problems. In our case, we used the so-called Expectation-Maximization algorithm to extract two Gaussian distributions from each experimental velocity distribution, which might be bimodal, and to obtain the mean velocity and velocity fluctuation RMS values for both extracted distributions.

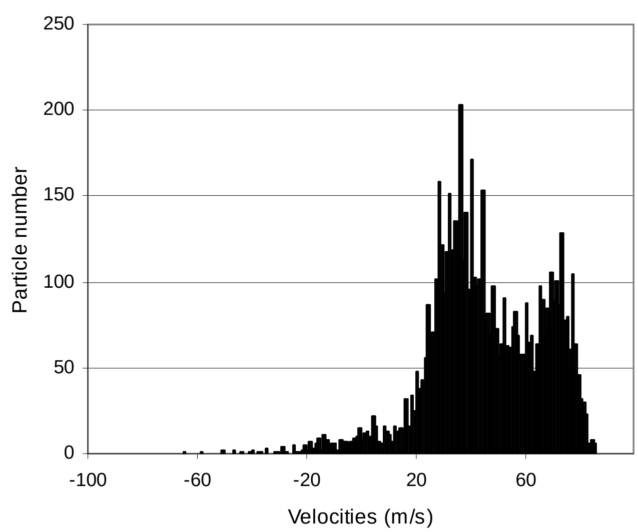

Fig. 13: Example of velocity distribution under reactive conditions for 0-5 μm particle diameter range, ZrO_2 and kerosene droplets, bi-modal distribution

This process was restricted to two Gaussian distributions, assuming the samples are clearly composed of two different types of population: Zirconia particles and small kerosene droplets.

Using this method we obtained a first population, called population #1, with a high velocity value and a second population, called population #2, with a low velocity value. Finally it was possible to identify, measurement point by measurement point, one of the population as the Zirconia particles, and the other as the small fuel droplets, by examining the size/velocity distribution of the whole sample of Zirconia particles and fuel droplets. Such a size/velocity distribution is shown in Fig. 14, for the velocity distribution presented in Fig. 13. The size information in Fig. 14 shows that the 30 m/s peak corresponds to small kerosene droplets, because they are contiguous to the larger droplets, which have the same velocity level. In the same way, the 70 m/s peak corresponds to the Zirconia particles, because at this velocity level, the size distribution does not extend beyond 10 micrometers. At this point, the gas phase velocity is therefore about 70 m/s. The accurate value is given by the average value of the Gaussian distribution of the first population extracted by the MIXMOD software.

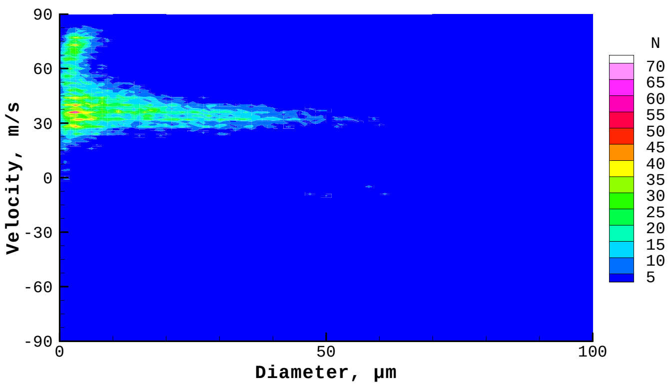

Fig. 14: Example of Size-Velocity distribution in reactive conditions, ZrO_2 and kerosene droplets, bi-modal distribution

With this method, Fig. 15 shows an example of velocity profile in the section close to the diffuser exit. On this plot, the whole sample, composed of Zirconia particles and small fuel droplets together (populations 1 & 2), is represented by solid black squares, population #1 (highest velocity value) by solid grey squares, population #2 (lowest velocity value) by empty black squares and the final gas phase velocity profile by a solid line. The plot shows that, close to the axis, the Zirconia particles, which seed the gas phase, are represented by population #2, then the gas phase is represented by the whole sample, then by population #1 and finally, at large radii, it can be noticed that all velocity measurements converge towards a unique value because the Zirconia particles and the few surviving small droplets have the same velocity. The curve shows also clearly that there is a velocity slip between the gas phase and the small fuel droplets from axis to radius 22 mm. The same behaviour was encountered in the 26 mm section. However, further downstream, at sections 56 and 116 mm, the velocity distributions looked monomodal and the extraction of two Gaussian populations was not pertinent. Going further downstream, because of evaporation and combustion, the proportion of small fuel droplets in the sample simply became negligible and they no longer had an influence on the sample velocity. The RMS values of the velocity fluctuations, which are not shown in this paper, are also available on demand.

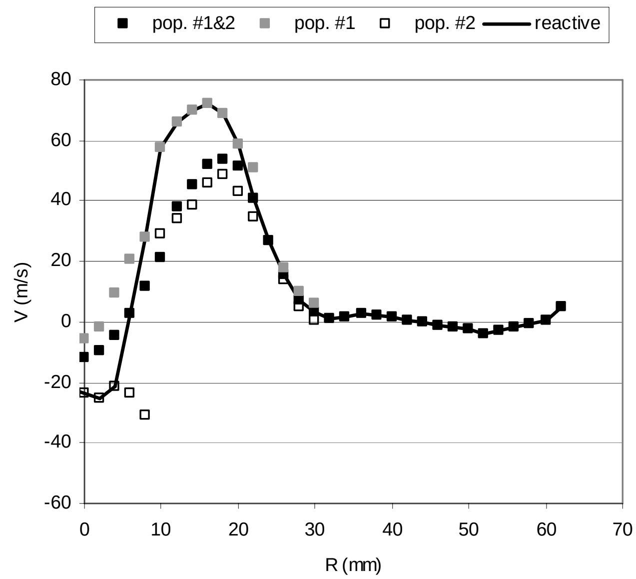

Fig. 15: Gas phase velocity profile (axial component) in reactive conditions in section 10 mm

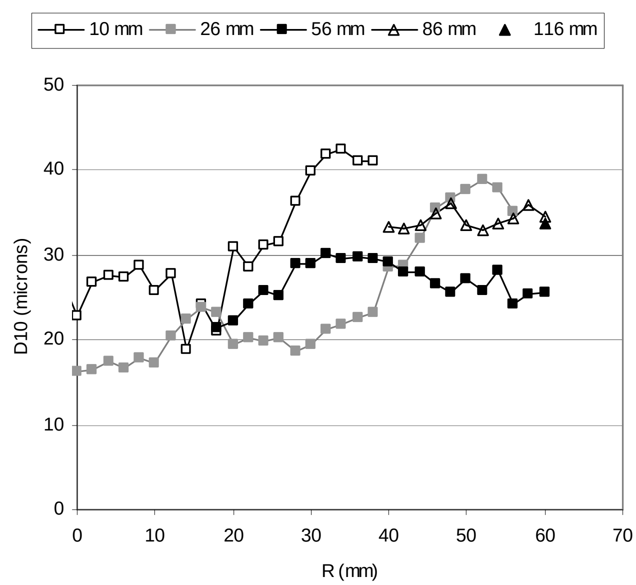

Fig. 16: Droplet mean diameter profiles under reactive conditions

Simultaneously with these measurements, the drop sizes and velocities (axial component) were acquired. These results are illustrated by the mean drop size profiles, Fig. 16 and the mean velocity axial component, Fig. 17, along a radius in 5 sections of the combustion chamber.

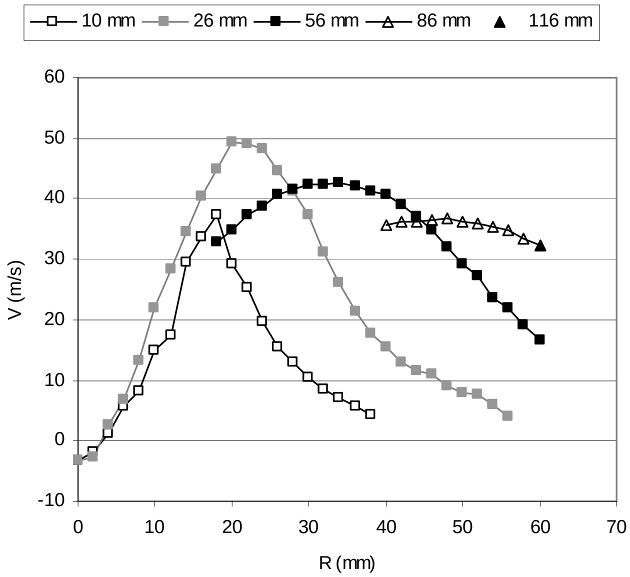

Fig. 17: Droplet velocity profiles (axial component) under reactive conditions

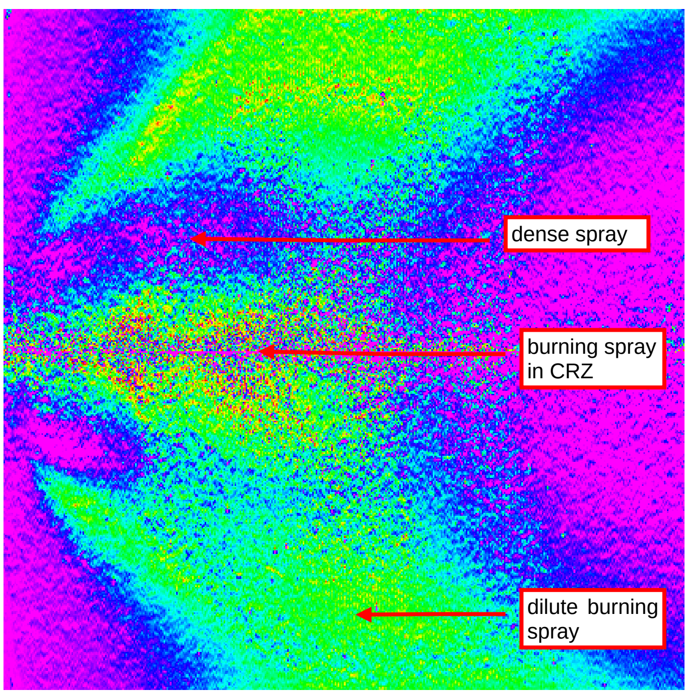

Fig. 18: Abel transform of the average flame visualisation (false colours)

Finally, a qualitative visualisation of the stabilized flame, which was perfectly blue, was performed through a lateral window of the combustion chamber. A high speed video camera was used in the visible range at a rather low frame rate (100 fps) and consequently a rather long exposure time (0.01s). An average picture was built from 391 snapshots and the resulting picture was processed by an Abel transform to obtain a longitudinal section of the flame, Fig. 18. The picture is square, 125x125 mm² for 430x430 pixels, and coloured, with purple, blue, green, yellow and red successively indicating an increasing intensity of the flame emission. Two combustion zones can be seen: an inner one in the central recirculation zone (CRZ) of the flow, surrounded by a large outer one downstream from the corner circulation zone. These combustion zones are separated by the dense part of the spray.

SYNTHESIS OF RESULTS

Before using this data base for the validation of spray combustion models, the experimental results have to be interpreted.

First, we can compare the velocity field of the gaseous and liquid phases, under reactive and non-reactive conditions. In four plates, Fig.19 (A,B,C & D) shows the profiles of the axial velocity of the gas phase under reactive and non-reactive conditions, and the one of the droplets under reactive conditions, for the four sections investigated during combustion (10, 26, 56, 116 mm).

In the 10 mm section, Fig.19A, close to the diffuser exit, the gas velocities in the central recirculation zone are equal for reactive and non-reactive conditions, which shows that combustion has no influence in the vicinity of the atomizer. In the same region, the droplet flow is very weakly influenced by the gaseous flow, with the droplets exhibiting zero velocity values whereas the gas phase exhibits large negative values. At larger radii (> 6 mm), in the jet region, the combustion accelerates the gas and expands this region, in comparison with the non-reactive flow. The droplets appear to keep the memory of their injection conditions with velocity values that are somewhat lower than the gas in the jet region (6<r<26 mm) and with higher velocity outside the jet (26<r<38 mm). In the outer recirculation zone, the reactive and non-reactive gaseous velocities are almost identical, meaning that, in this section, the recirculation is not fed by hot gases. There are no droplets in this zone.

In section 26 mm, Fig.19B, the gaseous back flow is much faster under reactive conditions than under non-reactive ones. Then, the developing spray combustion accelerates the gases over a large part of the width of the combustion chamber, from r=8 to 50 mm. Then, up to the wall, the back flow is again faster under reactive conditions than under non-reactive conditions, indicating that, at this location, the outer recirculation zone is fed with burnt gases. Concerning the liquid phase flow, the droplet velocities in the central recirculation zone do not evolve much between section 10 and section 26 mm, showing only a slight acceleration for the larger radii, 6 and 8 mm. This means that combustion does not yet have a large influence on the dynamics of the liquid phase in that zone.

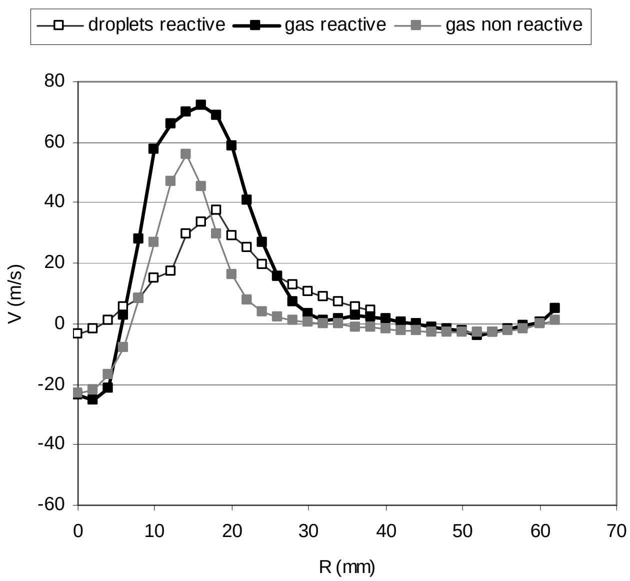

A -10 mm section

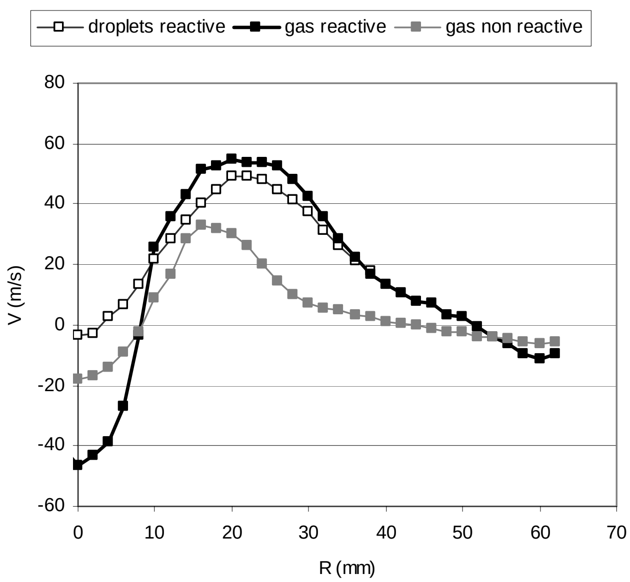

B - 26 mm section

In section 56 mm, Fig.19C, the gaseous back flow of the central recirculation zone again has a higher velocity under reactive conditions than under non-reactive conditions but both at lower levels. This behaviour is consistent with the radial expansion of the recirculation bulb from about 8 mm in section 26 mm to about 12 mm at section 56 mm. Then, at larger radii, the velocity profile under reactive conditions shows that combustion has filled the chamber almost up to the wall and that the outer circulation has almost ended at abscissa 56 mm. This is not yet the case for the non-reactive flow. As far as the liquid phase is concerned, there are no more droplets in the centre of the flow. Then, the comparison of liquid and gaseous velocities under reactive conditions shows that the droplets previously accelerated by the burnt gases do not decelerate as quickly as the gas phase (from r= 18 to 32 mm). Finally, at larger radii where the dynamic equilibrium between phases already existed in the previous section, this equilibrium is kept.

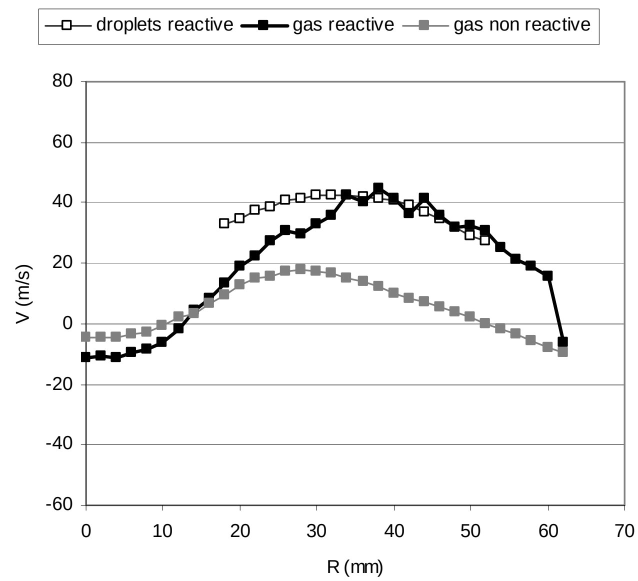

C - 56 mm section

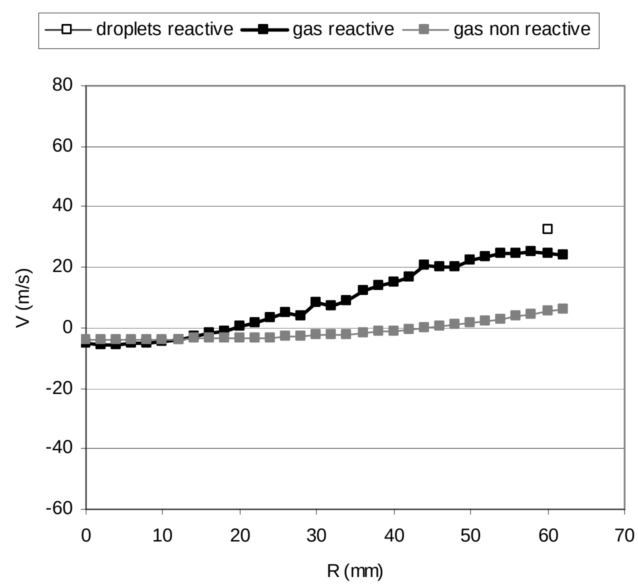

D - 116 mm section

Fig.19: Gas phase and droplet axial velocity profiles in the combustion chamber under reactive & non-reactive conditions

Finally, the same overall behaviour is observed for the gaseous flow in section 116 mm, Fig.19D, as in section 56 mm, but with lower amplitude extrema and with the disappearance of the outer recirculation zone under reactive and non-reactive conditions. In that section, droplets are observed only close to the wall.

Second, we can also compare the liquid phase data under reactive and non-reactive conditions in section 10 and 6 mm respectively. The arithmetic mean diameter (D10) and Sauter mean diameter (D32) profiles are plotted for both types of condition, Fig. 20. Let us recall that it is only possible to obtain reactive measurements over a distance of slightly more than a radius. This plot shows that the arithmetic mean diameter (D10) curves have the same evolution vs. radius, but quite different mean levels (about 33 micrometers under reactive conditions, much higher than 18 micrometers under non-reactive ones). Concerning the Sauter mean diameter (D32) curves, the mean levels are very close and, surprisingly, the behaviour is the contrary of the mean diameter one. These two opposite behaviours mean that, due to the combustion, the drop size distribution is strongly modified. The arithmetic mean diameter (D10) evolution shows that the smallest droplets disappear under reactive conditions and that the largest ones evaporate slightly, resulting in a narrower size distribution under reactive conditions than under non-reactive ones.

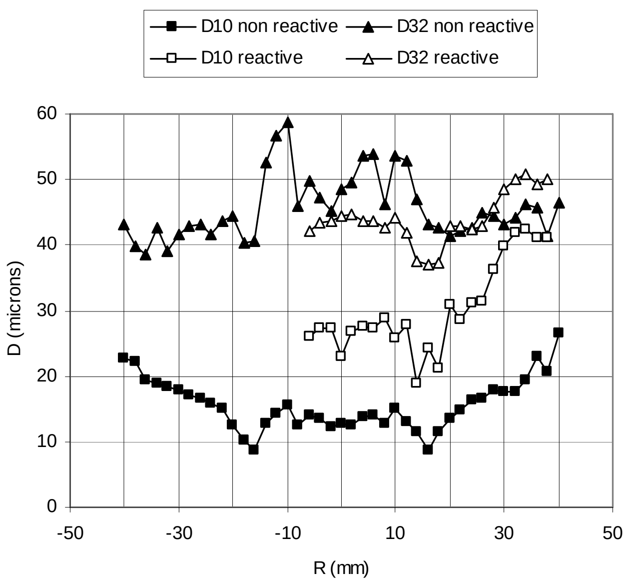

Fig. 20: Comparison of drop size profiles at 6 mm (non-reactive conditions) &10 mm sections (reactive conditions)

The comparison of the axial velocity profiles, Fig. 21, also shows a slight influence of combustion in that section. While the velocity extreme values are almost identical, we can observe a slight expansion of the hollow cone of the spray and an acceleration of the droplets outside of the cone.

Finally, Fig. 22 shows the superimposition of the gas phase velocity profiles, measured under reactive conditions, on the Abel transform of the flame visualisation.

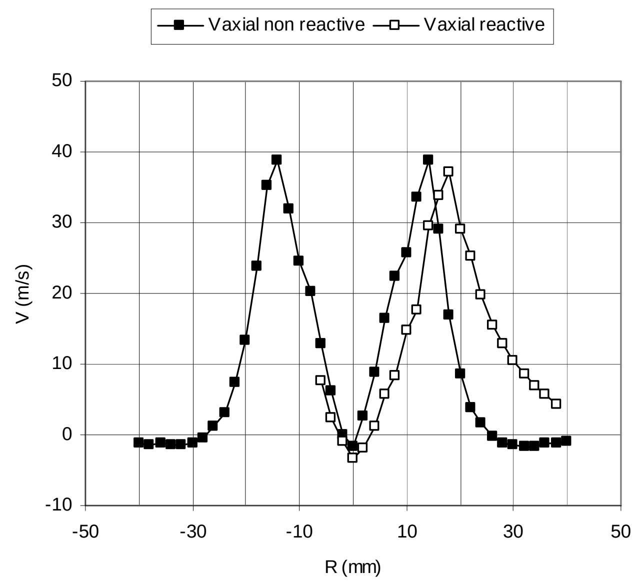

Fig. 21: Comparison of the mean drop velocity (axial component) under reactive & non-reactive conditions at section 8 mm

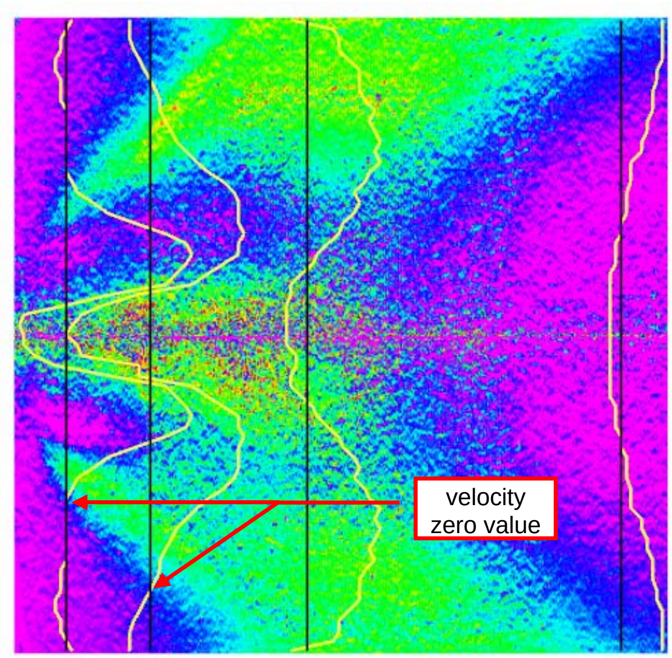

Fig. 22: Superimposition of the gas phase velocity profiles (yellow curves) under reactive conditions on the flame visualisation – the black lines are the measurement sections

In this plot, it is remarkable that, in the measurement sections 10 and 26 mm, the axial velocity takes the value zero precisely at the outer edge of the flame. This behaviour could be used as one of the criteria of the validity of the spray combustion models.

CONCLUSION

A reactive air/kerosene two-phase flow has been characterised in detail. The entry boundary conditions and the field characteristics of both phases required for the test of spray combustion models are available. Some additional information has also been acquired on the steady and unsteady cold flow and on the flame. The geometry and all the data are available from ONERA for research teams wishing to validate two-phase flow models under actual reactive and non-reactive conditions.

NOMENCLATURE

Main Scripts

D	[mm]	drop diameter
R, r	[mm]	radius
U	[m/s]	bulk velocity
V	[m/s]	velocity

Subscripts

h	horizontal
v	vertical

Acronyms

CERFACS	Centre Européen de Recherche et de Formation Avancée en Calcul Scientifique
CFD	Computational Fluid Dynamics
CRZ	Central Recirculation Zone
LDA	Laser Doppler Anemometry
MERCATO	Moyen Expérimental de Recherche en Combustion Aérobie par Techniques Optiques
ONERA	the French Aerospace Lab
PDA	Phase Doppler Anemometry
PRECCINSTA	PREdiction and Control of Combustion INSTAbilities for industrial gas turbines
PVC	Precessing Vortex Core
RMS	Root Mean Square
RX	LDA/PDA Receiver
TIMECOP-AE	Toward Innovative Methods for Combustion Prediction in Aero-Engines
TURBOMECA	A Company of the Safran Group
TX	LDA/PDA Transmitter

ACKNOWLEDGMENTS

This work received funding from the European Community through the projects TIMECOP-AE (Project # AST5-CT-2006-030828) and ONERA. This work reflects only the author's views and the European Community is not liable for any use that may be made of the information contained therein.

REFERENCES

[1] Barlow R.S., Frank J.H., 1998, “Effects of Turbulence on Species Mass Fractions in Methane/Air Jet Flames” 27th Symposium (International) on Combustion/The Combustion Institute, 1998, pp. 1087-1095.
[2] Schneider Ch., Dreizler A., Janicka J., Hassel E.P., 2003, “Flow Field Measurements of Stable and Locally Extinguishing Hydrocarbon-Fuelled Jet Flames“, Combustion and Flame 135, pp. 185-190.
[3] Meier W., Weigand P., Duan X.R., Giezendanner-Thoben R., 2007, “Detailed Characterization of the Dynamics of Thermoacoustic Pulsations in a Lean Premixed Swirl Flame”, Combustion and Flame 150, 2-26.
[4] Sankar SV., Buermann D H. and Bachalo W.D., “Simultaneous Measurements of Droplet Size, Velocity, and Temperature in a Swirl-Stabilized Spray Flame”, 1994, 7th Itnl. Symp. on the Appl. of Laser Techniques to Fluid Mechanics, Lisbon, Portugal
[5] Behrendt T., Heinze J. and Hassa C., “Experimental Investigation of a New LPP Injector Concept for Aero-engines at Elevated Pressures“, ASME/IGTI turbo Expo GT2003-38444.
[6] Becker J. and Hassa C., “Experimental Investigation of Spatial and Temporal Aspects of the liquid Fuel Placement in a Swirl Cup at Elevated Pressures“, ASME/IGTI turbo Expo GT2004-53524.
[7] Russo S., Gomez A., 2006, “Physical Characterization of Laminar Spray Flames in the Pressure Range 0.1-0.9 MPa”, 2006, Comb. & Flame 145, pp. 339-356.
[8] Chrigui M., Sadiki A., Janicka J., Hage M. and Dreizler A., 2009, “Experimental and Numerical Analysis of Spray Dispersion and Evaporation in a Combustion Chamber”, Atomization and Sprays, 19(10), pp.929-955.
[9] Lecourt R., Bismes F., Heid G., “Experimental Investigation of Ignition of an Air-Kerosene Spray in Altitude Conditions”, ISABE-2009-1235.
[10] Sanjosé M. et al., “LES of two-phase reacting flows“, Proceedings of the Summer Program, 2008, pp. 251-264, Center for Turbulence Research, NASA AMES, Stanford University, USA.
[11] Biernacki C., Celeux G., Govaert G.,. Langrognet F, 2006, “Model-based cluster and discriminant analysis with the mixmod software”. Computational Statistics and Data Analysis 51/2, pp. 587-600.

